*Sādhanā* (2020)45:138
https://doi.org/10.1007/s12046-020-01367-5



# Development of an experimental set-up to measure sound absorption coefficients of porous materials

MANISH RAJ, SHAHAB FATIMA* and NARESH TANDON

Industrial Tribology, Machine Dynamics and Maintenance Engineering Centre (ITMMEC), Indian Institute of Technology Delhi, Hauz Khas, New Delhi 110016, India
e-mail: manishraj.iitdelhi@gmail.com; fatima@iitd.ac.in; ntandon@itmmec.iitd.ac.in

MS received 5 April 2019; revised 16 January 2020; accepted 14 February 2020

**Abstract.** This paper discusses the practical aspects of data acquisition and signal processing techniques involved while developing an impedance tube. Microphones, data acquisition systems, set of speakers were carefully selected, calibrated, and assembled as one unit. The raw time signal is acquired through a Virtual Instrument (VI) developed in LabVIEW, and the mathematical equations involved in the process are implemented in MATLAB R 2017a. Important considerations involved in these processes have been thoroughly discussed in the paper. The final results contained outliers that were removed by the application of digital filters. The results obtained from the application of different types of digital filters are shown, discussed, and the best combination of filters has been selected. This combination results in a robust and efficient method with an improved low-frequency response (< 250 Hz) which, in a standard commercial impedance tube, was achieved by altering the microphone spacing. The validation was performed by conducting experiments on a blank tube, melamine foam, glass wool, and comparison were made with the result obtained on the set-up of a leading manufacturer, and with the ones reported in works of literature. They show a good match between them which completes the validation.

**Keywords.** Virtual instruments; porous materials; impedance tube; ASTM E 1050; transfer function technique; noise reduction coefficient.

## 1. Introduction

Rapid industrialization has led to the development of new types of machinery and comfort components that are aimed at easing out human life. They serve their purpose pretty well along with some untoward upshot, one of those being radiating some amount of sound. Mass usage of these have a cumulative effect which needs to be dealt with, and this led to the notion of unwanted sound to be known as noise, which is considered to be a source of pollution. It has severe effects ranging from general annoyance to high blood pressure [1]. New ways to tackle this form of pollution is being devised, with the introduction of tighter norms. Noise is emitted from a source, travels through a medium, and finally reaches a receiver which becomes a victim. It can be reduced by some design changes of the source, or by isolating the victim, which are the extreme options and may not always be desirable or feasible. Hence, noise control in the path when the sound is traveling from source to victim needs to be exercised [2]. This is achieved by the introduction of sound-insulating material between source and victim. Sound absorbing material is used for acoustical comfort by controlling the reverberations from a hard reflecting surfaces which can easily be observed in any auditorium, multiplexes, theaters, lecture hall, etc. The performance of these sound absorbers is quantified by the term sound absorption coefficient (SAC) which represents the ratio of sound power not reflected by the material to that of the incident sound power. It varies with frequency as the same material behaves differently when incident by the sound of different frequencies. This parameter may be estimated at an oblique incident of sound which is more realistic in nature or normal incident of sound which provides a good platform for comparison between the performance of different sound absorbers. The former needed reverberation chambers for measurement. These were a separate infrastructure in itself in the form of a sound generator and a sound receiver room. These rooms needed to be separate from the attached buildings to avoid flanking's transmission [3], and this boosted the cost involved. This motivated the researchers to develop an impedance tube which estimated the sound absorption coefficient (SAC) of material under normal incident of sound. This approach reduced the cost significantly, but it remained high on an absolute scale which strictly limited the research base on acoustic materials. The initial design of the impedance tube measured the sound absorption of a material by a

*For correspondence
Published online: 27 May 2020

traveling microphone in which the response at each frequency was evaluated individually [4]. It was a time-consuming process that was overcome by the introduction of the transfer function technique [5] which used two microphones and estimated the broadband response in a single attempt. There are many works of literature available for the physical design which discusses the appropriate dimension and vibroacoustic response of the tube [6–12]; still, there existed a fair gap which needed to fill up like addressing the issues concerned with upper working frequency limit, low-frequency response, etc. [13, 14]. The tube wall attenuation earlier used to be ignored severely affected the low-frequency response which was highlighted by [15], and a solution was suggested which recommended increasing the microphone spacing for low frequency; this needed three slots in a single tube and the microphone spacing was adjusted accordingly. So, overall there used to be two different tubes and four different microphone spacing. Altering the microphone spacing repeatedly in a tube disturbed the whole system and made the whole process time-consuming. The issues related to data acquisition, signal processing, and mathematical equations implementation also remained unclear. This paper addresses these issues and extensively discusses the concerns involved in the development of an impedance tube unit as per the standard ASTM-E-1050. Data is acquired by using the LabVIEW platform integrated with two National Instruments (NI) compact data acquisition (c-DAC) chassis. It is a quite user-friendly platform that allows customization of all the acquisition channels [16, 17]. Researchers have found it to be very efficient from a simple application such as data acquisition and spectrum analysis of the acquired signal to complex applications like remote access to a laboratory or even in the launch of magnetic projectiles which used feedback from the acquired signal [18, 19]. The acquired signal has been processed, and mathematical operations as suggested by the standard, have been implemented on it. The spectrum of sound absorption coefficients obtained are further smoothened and outliers present in it are removed by the application of digital filters using MATLAB. There are several algorithms available for outlier removal and smoothing of the signal such as sliding window outlier removal, the minimum median of squares of error, using neural network, etc. [20–22]. The inapt points have been removed by several filters, and the most appropriate one is chosen for the final result. The methodology followed was repeated for different conditions, and the final results have been compared to the results obtained from commercial impedance tubes and those reported in the literature showed a good match, and thus the developed impedance tube set up was validated.

## 2. Component selection and assembly

The layout of the component fabricated, selected, and assembled as per ASTM-E 1050 is shown in figure 1. The whole system is associated with a tube, which needs to be considered first. It has to be seamless and smooth, which offers minimal resistance to the propagation of sound. Considering all these guidelines, an acrylic tube is selected for the desired work. This material has an additional advantage of being transparent which enables an operator to keep a watch on the positioning of the microphone. It has been used in the past with an acceptable result [6, 23]. The dimensional parameters of the tube involve its diameter (D), length from speaker to the nearest microphone (L), the spacing between the microphones (S), distance from test material to the second microphone, (*l*). All these are governed as per the standard, which takes into consideration the physics of the phenomenon in the tube. The diameter is limited by the upper working frequency of the tube, by the empirical equation (1).

$$D < \frac{0.586c}{f_u} \tag{1}$$

The constraint of equation (1) suggests the usage of a tube of smaller diameter for a higher upper-frequency limit. A tube of smaller diameter restricts the planarity of sound waves at low frequencies when the wavelength is considerably higher. This is resolved by using two different tubes for the diverse upper working frequency range. A large tube of diameter 100 mm is designed to work till 2000 Hz, and another tube of diameter 29 mm is designed to work till 7000 Hz. The spacing between the microphones (S) governs the lower working frequency of the tube. As the two mics are mounted side by side, there has to be a considerable phase change at these two locations. Hence, it is suggested to keep the spacing greater than one percent of the wavelength at a lower frequency. One more guideline from the standard is to keep the microphone spacing $S << c/2f_u$. Considering these, the spacing between microphones is held at 50 mm in the large tube and 25 mm in the small tube, which corresponds to a lower working frequency of around 70 Hz and 140 Hz respectively. One

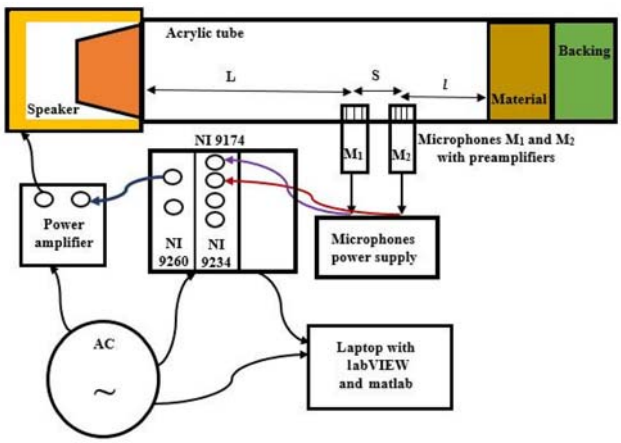


**Figure 1.** The layout of the developed impedance tube.

of the vital assumptions in an impedance tube is that the sound waves are planar, which may not always be the real situation as some nonplanar waves may be generated from the sound source. This nonplanarity fades out at a length of about three times the tube diameter, and this phenomenon governs the length of the tube. The length of the large tubes in this study was kept around 600 mm, and the smaller tube is around 300 mm. The distance between the test material and the second microphone is governed by the type of surface of the test specimen. If the surface is wedge type, the sound waves reflected from the peak reaches the microphone earlier than the ones reflected from other portions, which degrades the signal to noise ratio. Hence, it has to be such that any effect of the non-flatness of the test specimen is minimized on the reflected waves, and the recorded signal contains the maximum signal and minimum noise. It is suggested to be one half of the tube diameter, one tube diameter and two times the tube diameter for a flat surface, nonhomogeneous surface and asymmetrical surface respectively. This distance is kept at 200 mm in a large tube and 50 mm in a small tube.

Microphones are of free field and pressure field types. The former is used in an open area in the absence of any significant reflections of the sound waves, and the latter is used in the presence of a large amount of reflection, such as in a duct or tube. Hence a pressure field microphone, B&K type 4166, is selected for the intended application. As it's diameter is of half an inch, the maximum working frequency limit of the tube is restricted at 5600 Hz as per the standard (ASTM E-1050). It is connected to a preamplifier, B&K type 2619. The polarization voltage of 200 Volts needed is provided by a dual-microphone power supply, B&K type 5935. Its output goes into the data acquisition (DAQ) system. The DAQ system has to perform the acquisition of the microphone signal, and simultaneously it has to send an output signal to the speaker. To synchronize both these processes, a National Instruments (NI) chassis 9174, which has four slots to perform operations simultaneously, is selected. For acquisition, the first slot is fitted with NI 9134 Sound and Vibration card and a digital output card NI 9260 is fitted in the other slot. It has been verified that the result is independent of the positioning of these two cards in chassis. The effect of external noise leakage into the system is minimized by keeping the sound level in the tube to be higher than the ambient noise by 15 dB. The digital output card has its maximum output voltage of 2 volts, which needs further boost up to achieve this. Hence, a power amplifier, B&K type 2706 with adjustable gain control, is used for this purpose. Finally, a driver speaker is selected such that it has a flat response in the operating frequency range. The chosen speaker has a flat response in the region 50-5500 Hz. The standard also suggests having a porous absorber lining inside its cover to avoid resonance of the air column into the tube. It is achieved by pasting a glass wool lining inside the speaker holder. So, keeping a safety factor, the large tube operates in the range of 100-2000 Hz, and the small tube operates between 1800-5000 Hz.

Microphones are checked with an acoustic calibrator (CEL-284/2) every time before the experiment starts. To ensure a correct result, the other components need to be checked for their accuracy. The cables used to connect different parts may play a spoilsport on malfunctioning. All the cables involved are checked for their continuity and leakage using a multimeter. The speaker, power amplifier, NI 9260, and NI 9234 are checked for their accuracies. A pure tone was sent at a lower, central and upper frequency of $1/10^{th}$ Octave, and satisfactory results were obtained. This omitted any possibility of any meddling with the signals by any subcomponents. The final assembly with all the subcomponents is shown in figure 2.

## 3. Methodology

The transfer function between the sound pressures recorded at the first microphone and second microphone is estimated as the ratio of their cross power spectrum $(G_{12})$ and auto power spectrum $(G_{11})$. The calibration factor of the tubes due to channel mismatch is evaluated before proceeding with measurements on the actual material. A highly absorptive sample of glass wool is placed in the sample holder to estimate the transfer function of the tubes in

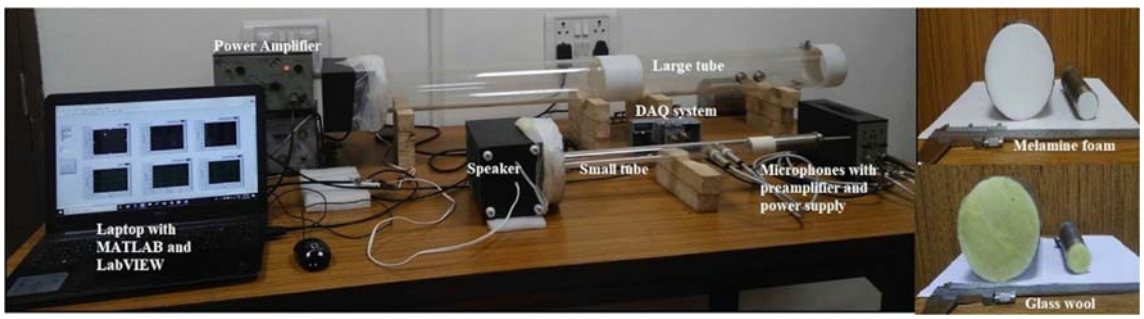


**Figure 2.** View of developed impedance tube set up with samples.

standard configuration ($H^I$). Microphones are then swapped with each other to determine the transfer function in swapped configuration ($H^{II}$). The calibration factor is given by equation (2).

$$H_c = \sqrt{(H^I \times H^{II})} \tag{2}$$

The absorptive sample is then replaced with the sample to be tested, and its transfer function is estimated by equation (3).

$$H' = \frac{G_{12}}{G_{11}} \tag{3}$$

This is divided by the calibration factor to obtain a corrected transfer function, as expressed in equation (4).

$$H = \frac{H'}{H_c} \tag{4}$$

The complex reflection coefficient (R) is calculated by equation (5).

$$R = \frac{H - e^{-jks}}{e^{jks} - H} e^{j2k(l+s)} \tag{5}$$

k, the complex wavenumber is estimated by equation (6).

$$k = k' - jk'' \tag{6}$$

The real component of wavenumber is estimated by equation (7).

$$k' = \frac{2\Pi f}{c} \tag{7}$$

The complex component of wavenumber, known as attenuation constant, is estimated by equation (8).

$$k'' = 0.02203\sqrt{\frac{f}{cD}} \tag{8}$$

Finally, the sound absorption coefficient ($\alpha$) is evaluated by equation (9).

$$\alpha = 1 - |R|^2 \tag{9}$$

Melamine foam is a widely used acoustic material that has been extensively studied by the researchers [19]. It is easily available, and its results can be easily validated. This was the motivation in choosing this material for endorsement of the developed set up. Two 30 mm thick test samples of diameter 100 mm and 29 mm were procured from Alfa Acoustics (Pune). Glass wool is one of the best sound-absorbing material and hence it is selected as the highly absorptive material required to estimate the calibration factor. It was procured from the local market. 12 layers of glass wool, each having a thickness of 10 mm, are piled up to make a highly absorptive sample of diameters 100 mm and 29 mm, respectively. Some properties of both these materials as provided by their respective suppliers are listed in table 1.

**Table 1.** Properties of the melamine foam and Glass wool sample used for the experiment.

| Parameter | Melamine foam | Glass wool |
|---|---|---|
| Bulk density (Kg/m$^3$) | 9 | 24 |
| Airflow resistivity (Ns/m$^4$) | 11500 | 6000 |

## 4. Data acquisition

Data acquisition (DAQ) is performed by designing a block in the LabVIEW software, which communicates with the DAQ system (hardware). Blocks can be made using DAQmx pellets or DAQ Assistant pellets. The former one is quite flexible in which channel is created, configured as per the application, and this type is better for single-channel data acquisition or independent multiple channel acquisition. DAQ Assistant pellets are used for complicated applications like the one needed in this research work where three channels (2 channels for reading the data and one channel for writing the data) operate in unison, along with an additional complexity of difference among microphones sensitivity.

A while loop, which has an option of terminating with a stop button is formed, and two DAQ assistant lines are formed and shown in figure 3. The First line for writing the data through NI 9260 and another for reading through NI 9234. The first line gives an output of uniform white noise which is played through the speaker into the tube. White noise can be provided in many ways, by using an express VI in which uniform white noise is added to a sine signal, and then the fraction of signal is reduced to zero, leaving only white noise. The best method is to utilize waveform pallet and then to define its parameters. The second line receives input from both the microphones through a single DAQ assistant, which is later split into two different paths, using a split signal option. The data inside the loop is displayed in a chart indicator that records the signal from start to end or in a graph indicator which shows the data of the last iteration of the loop.

The waveform is generated, played, and received back through a single interface involving much hardware of different specifications. This requires the generation and acquisition in a balanced manner in the absence of which error involving buffer size and system clock speed arises. In this case, the system in the application is balanced out when the loop operates once in 5 seconds. The loop terminates when it is stopped with the STOP button, or there is some error or when the predefined time is over. In this application, the terminating time is kept at 15 seconds and the

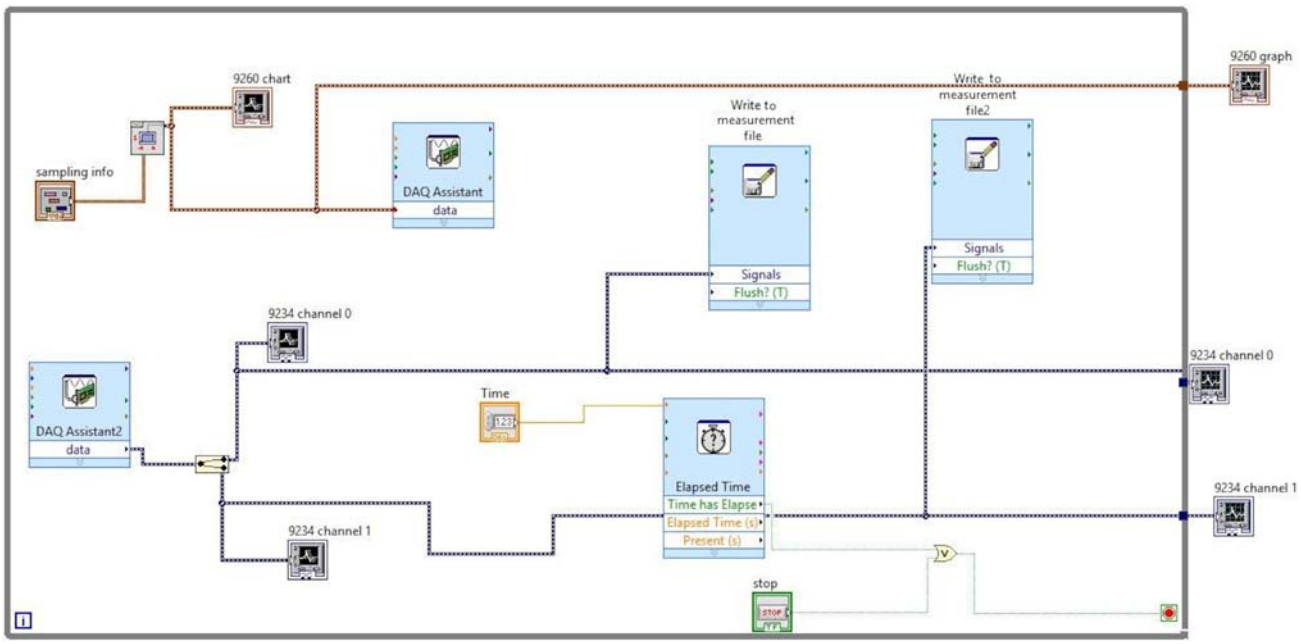


**Figure 3.** Block diagram of VI for data acquisition.

sample rate is kept as $2^{14}$. Whole VI operates in a while loop which is similar to a "do while" loop in other programming languages (C-language). This loop by its very property terminates after execution when the condition of termination is met. It is worth noting that the chart indicator, in this case, records the data for 20 seconds, 15 seconds for the pre-decided time and 5 seconds of data is for the last round after which it terminates. These chart data are recorded in an excel sheet and are used for further implementation of mathematical equations and processing. Figure 3 shows the block diagram of the VI in its simplest form which is developed for the acquisition and figure 4 shows its front panel.

A similar procedure is repeated for the other tube, and recorded data is then imported in MATLAB for further processing. The time-domain recorded at both the microphones in both the tubes is shown in figure 5. Before proceeding any further, the first work is to ensure that these time signals recorded are correct. There are several sources of error involved in the system such as power amplifier clipping, microphone channel overload, the air gap between the sample holder and tube, the air gap between microphone preamplifier and holder. These errors if unattended lead to garbage results like the negative value of SAC or SAC value higher than one by many folds. The microphones are closely spaced and standing waves are formed in the tubes which are in a steady-state. Any significant difference in the appearance of the signal signifies the presence of some error in the system which needs to be identified and resolved. The time-domain signal must look similar to its neighboring signal at any given time. An example of an incorrect signal during which the overload of microphone channels was recorded is shown in figure 6 in which it is worth noticing the amplitude of the signal between 1 second and 2 seconds which differs significantly with their neighboring ones.

## 5. Signal processing

Glass wool samples are placed in the sample holder and sound pressure is recorded at both the microphone locations. The microphone positions are swapped and sound pressure is recorded again. These values are used to compute the channel correction factor as stated earlier in section 3. Glass wool is replaced by Melamine foam and sound pressure is recorded again, similar to figure 5. The standing wave spectrums formed in the tubes with melamine foam is shown in figure 7. It contains information from zero till Nyquist frequency. The larger tube operates between 100-2000 Hz and the small one in the range of 1800–5000 Hz. A careful look at these plots and comparing the data among the sub figures, it is observed that the energy content at low frequencies is comparatively larger than the ones at high frequencies. This observation provides some idea of the absorption behavior of the material in a way that this material may turn out to be a good absorber at higher frequencies, which is typically the case for sound absorbers [24, 25].

The extra data outside the working range needs to be omitted to save the processing time involved in the computation. This is achieved by a bandpass filter, which is of

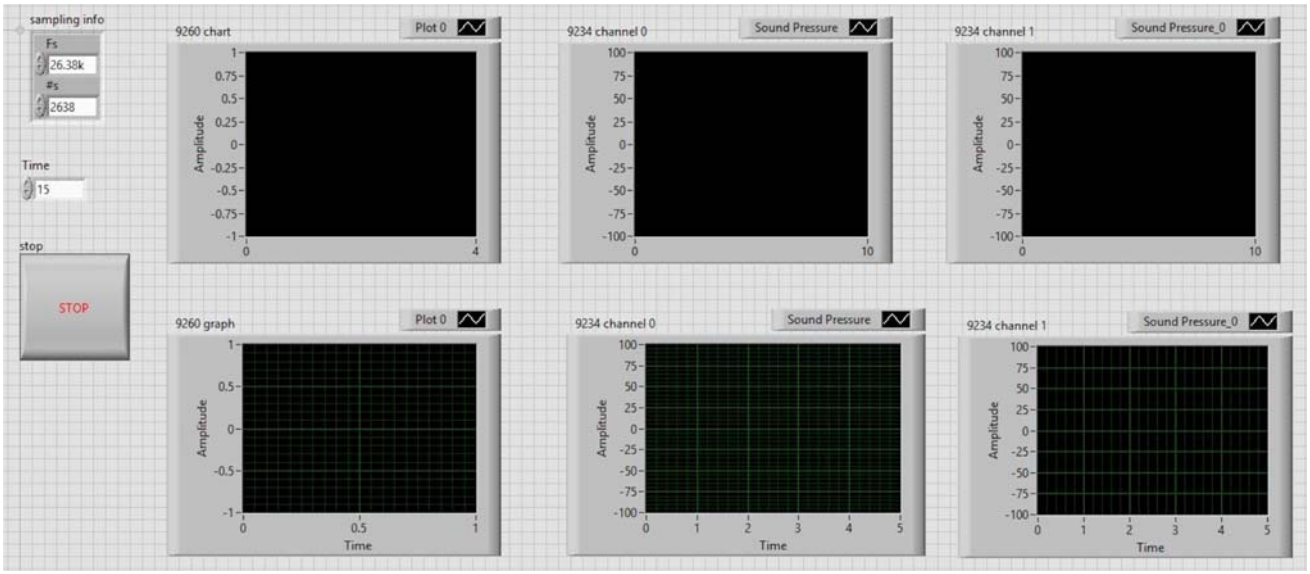


**Figure 4.** View of the front panel of VI for data acquisition.

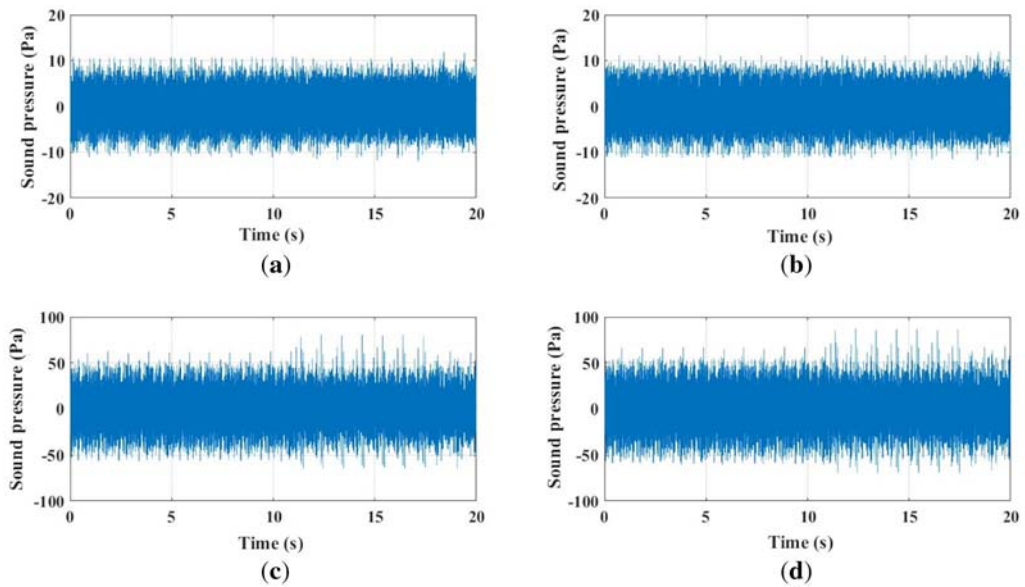


**Figure 5.** Time signal of Melamine foam (a) Mic 1 (large tube). (b) Mic 2 (large tube). (c) Mic 1(small tube). (d) Mic 2 (small tube).

Infinite Impulse Response (IIR) type or Finite Impulse Response (FIR) type. FIR filters work just like convolution and are more powerful but need more computation time. They also introduce some transient effect into the signal, which changes the signal length. This needs to be avoided in this case to reduce the chances of error while calculating the cross power spectrum. IIR filters are very efficient, respond just like analog filters without altering the data points in the passband range. Butterworth IIR filter is used in this work which is quantified by its orders. The order of a filter states its ability and efficiency to remove the unwanted information from a signal. The response of a Butterworth filter with different orders is compared in figure 8. As the order is increased from five to ten, the response at low cutoff frequency gets distorted which implies it is good for lower-order tapping. Comparison of the filter response with orders 3 and 5 shows the latter to have less transition band which ensures better anti-aliasing characteristics. Thus, an IIR filter with order five has been selected to filter out the unwanted information from the time domain signal.

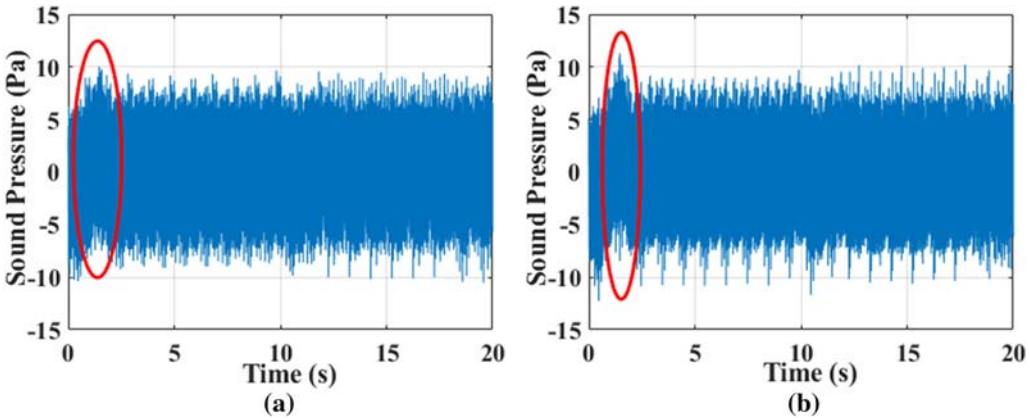


**Figure 6.** Distorted signal acquired while performing tests on Melamine foam, the portion which differs from its neighboring signals is encircled. (a) The signal at Mic 1 (large tube). (b) Signal at Mic 2 (large tube).

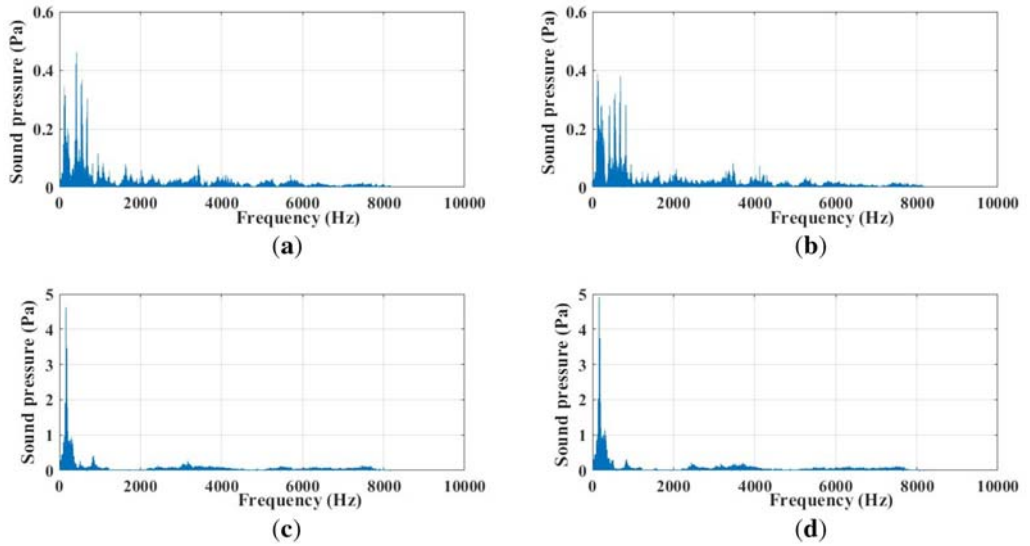


**Figure 7.** The spectrum of standing waves (a) Large tube (Mic 1). (b) Large tube (Mic 2). (c) Small tube (Mic 1). (d) Small tube (Mic 2).

The filtered and unfiltered signal in time and frequency domain are shown in figure 9, in which some energy has been filtered out from the signal which corresponds to the non-desired region. To ensure that the filter has not altered the passband signal, the filtered and unfiltered signals in the frequency domain are also shown in the same figure. It can be noted that the amplitude in the frequency domain for the non-pass band region has diminished to zero, and the location of the peak in the passband is precisely the same in the filtered and unfiltered signal. This confirms the successful working of the appropriately tuned selected filter and allows us to proceed further with the filtered signal.

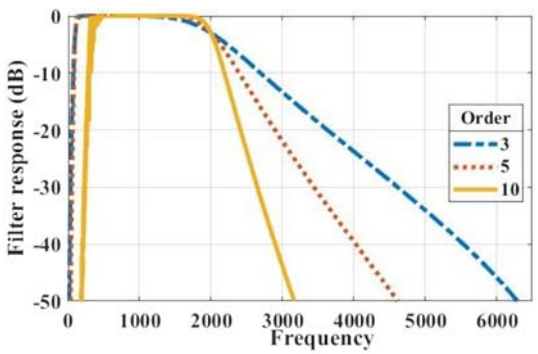


**Figure 8.** Effect of filter order on response in an Infinite Impulse Response (IIR) filter.

Mathematical equations are implemented on these filtered signals to obtain the values of SACs. Figure 10(a) shows the SACs for the bigger tube, which is valid for a frequency range of 100-2000 Hz. Similarly, figure 10(b) shows the SACs obtained for the smaller tube which operates in the frequency range, 1800–5000 Hz.

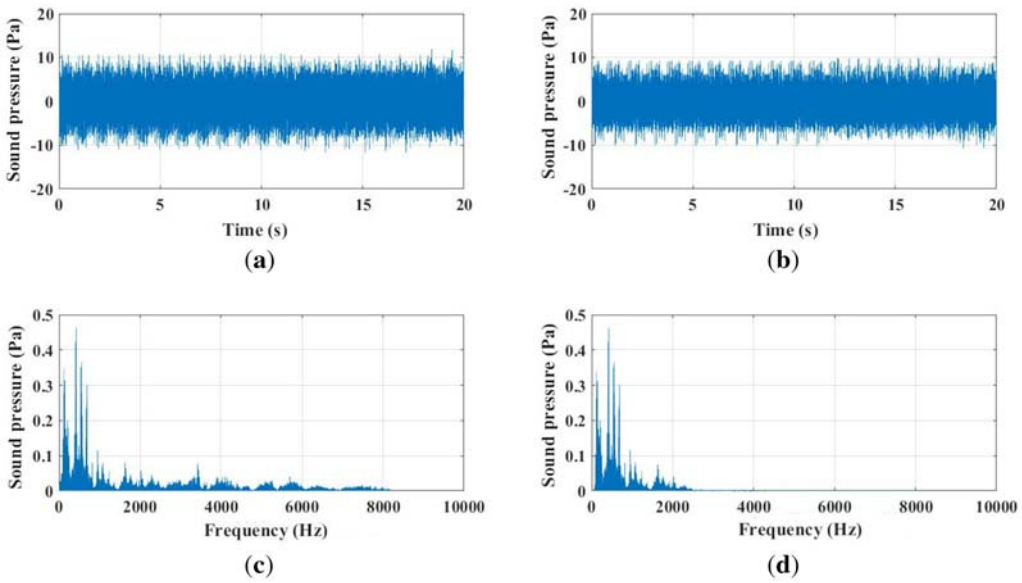


**Figure 9.** filtered and unfiltered signal a) Unfiltered time signal. (b) Filtered time signal. (c) Unfiltered spectrum. (d) Filtered spectrum.

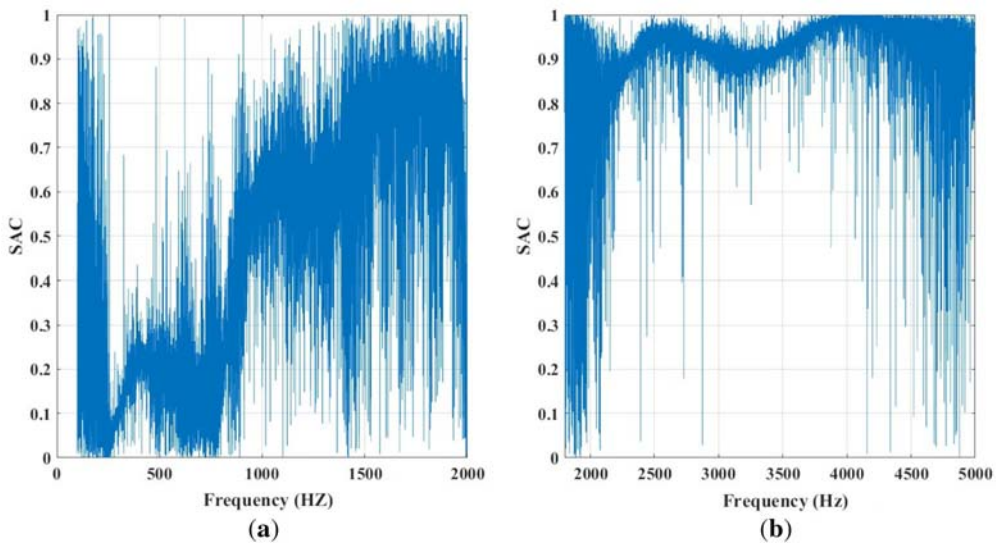


**Figure 10.** Sound Absorption Coefficients (SAC) obtained from the two different tubes (a) Large tube. (b) Small tube.

The individual results obtained from both the tubes for diverse frequency range needs to be assembled into one. For this, the results of the larger tube are accepted as it is in the frequency range of 100-1800 Hz. Similarly, the results of the smaller tube are kept as it for the frequency range of 2000-5000 Hz. The frequency range of 1800-2000 Hz is kept as a common region and the average results from the two tubes in this region are considered. The results of both these tubes are combined into one is shown in figure 11.

## 5.1 *Application of digital filters to remove outliers*

A clear absorption trend is not observed in Fig. 10 and Fig. 11. This contains a lot of noise in the form of outliers that needs to be filtered and smoothened out. It is achieved by the application of digital filters.

5.1a *Hampel filter*: Hampel filter is a decision-based filter that recognizes the crude pattern and removes multiple outliers without disturbing the original sequence in a signal [26, 27]. It cleans out a signal using the median absolute

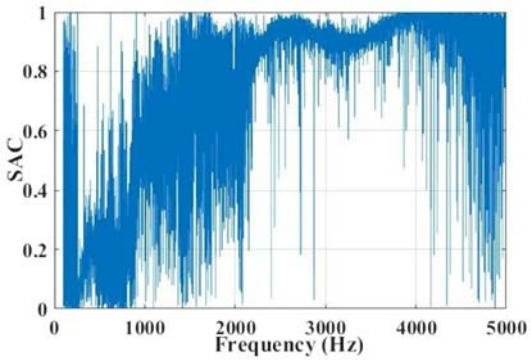


**Figure 11.** Sound absorption coefficients obtained from both the tubes combined.

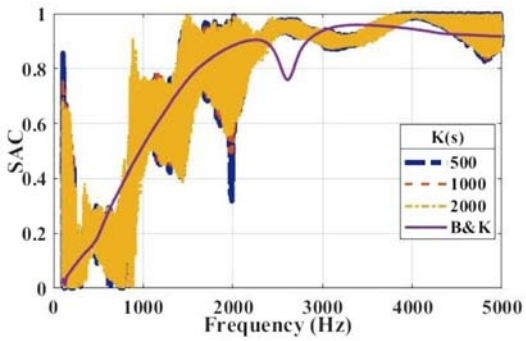


**Figure 12.** Sound absorption coefficient obtained by changing the window length, K(s) in a Hampel filter compared to the results obtained from a commercial B&K impedance tube.

deviation technique in which the data points are divided into smaller windows of length K(s) which slides from start to end. A particular data point is replaced by the window median if its absolute difference from the window median differs by the median absolute deviation scale estimate multiplied by a factor (Sigma) and 1.4826 [28–30]. Hampel filters become equivalent to the median filter when this factor is zero. K(s) and Sigma (s) are the two varied variables. Data points of 500, 1000, and 2000 are considered in a window in figure 12 in which a significant removal of outliers is noted when the window length is increased from 500 to 1000. Further increase in window length from 1000 to 2000 does not have any significant effect. Thus, 1000 data points are considered for further processing to get an optimal processing time. By the definition of the Hampel filter, it appears that lower sigma value may fetch better results. Sigma is usually kept at 3 in the results of figure 12, and it is changed to 0.5, 1 and 2 for 1000 data point windows. The results are shown in figure 13. The outliers get a significant combing effect with a decrease in the value of sigma without much difference in processing time, and thus

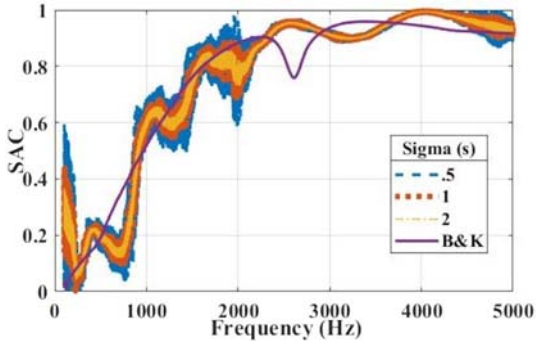


**Figure 13.** Sound absorption coefficient obtained by changing the filter factor (Sigma) in a Hampel filter compared to the results obtained from a commercial B&K impedance tube.

sigma value of 0.5 is considered for further refinement of the results.

5.2b *Savitzsky-Golay filter*: This filter was first used as low pass FIR filters to obtain information from the signal of a noisy chemical spectrum analyzers, and the results were very impressive [31]. Its working is similar to the curve-fitting approach. Still, it fetches a better result than the regression formulae. The entire data set is divided into smaller frames, the length of which has to be odd to maintain a central point. It then uses a minimum least squared error technique to fit a curve of given order across the length of the frame, which then slides across the whole dataset [32, 33]. It refines highly noisy data and preserves their shape, due to which it is highly used in biomedical instruments such as electrocardiogram machine [34]. The frame length and order of the polynomial to be fitted are varied on the noisy signal, and the results are compared, as shown in figure 14. It is observed that the waviness of the filtered signal increases with an increase in the filter order. An increase in frame length improves the low-frequency response significantly. An increase in frame length also increases the computation time, and hence a trade-off is there between computation time vs. accuracy.

## 6. Combined filtering and validation

Both the filters mentioned in the previous sections have improved the results individually. Hampel filter provides a combing effect of the outliers, and the Savitzsky-Golay filter provided the smoothing effect. The results obtained can be further improved by the combined effect of combing and smoothing. The noisy data in figure 11 is filtered by the combination of best performing Hampel filter (K(s) = 1000, Sigma (s) = 0.5) and Savitzsky-Golay filter (Order = 1, Frame length = 20001). It remains a curious point whether any difference inthe final result is observed when the filters are first applied on the results of individual tubes (figure 10) and then assembled for the full working

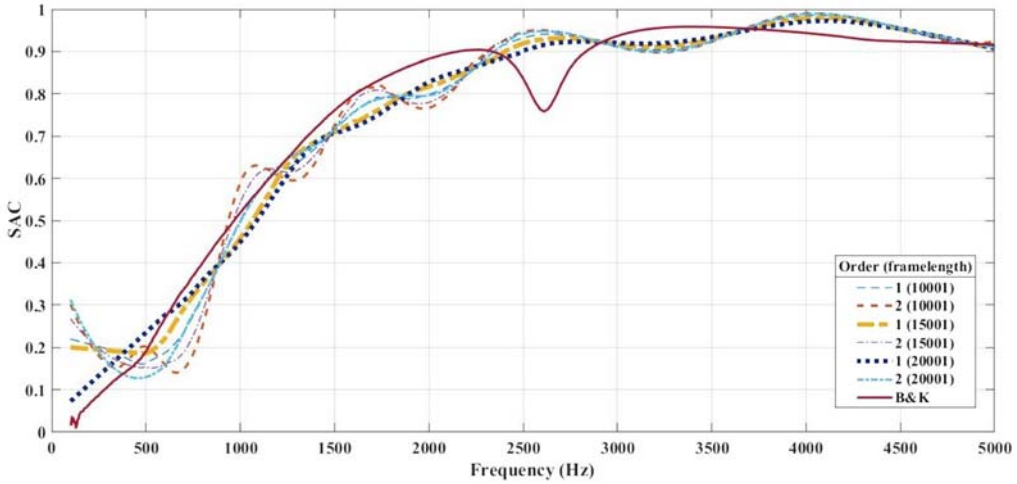


**Figure 14.** Sound absorption coefficient obtained by changing the order and frame length in a Savitzsky-Golay filter compared to the results obtained from a commercial B&K impedance tube.

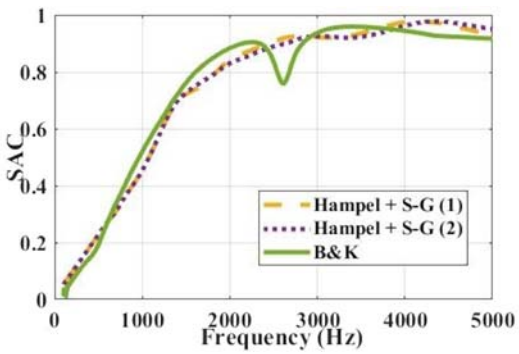


**Figure 15.** Sound absorption coefficient obtained by the altering the position (before assembling the result obtained from individual tubes and after assembling the result obtained from different tubes) of application of Hampel + S-G filter compared to the results obtained from a commercial B&K impedance tube.

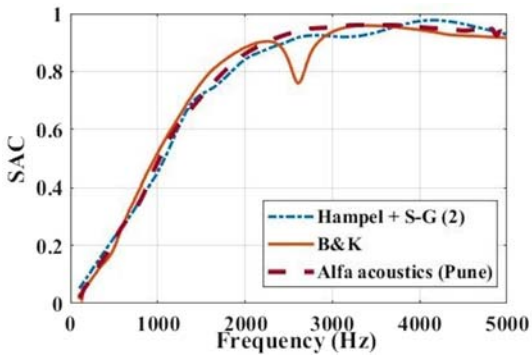


**Figure 16.** Sound absorption coefficient obtained by the best performing filters compared to the results obtained from a commercial B&K impedance tube and the result provided by the supplier of the Melamine foam.

frequency range or application the filters on the assembled values of SAC (figure 11). The filter for the former type is named Hampel + S-G (1) and for the latter, it is named Hampel + S-G (2). Both the results compared with the one obtained in a standard commercial tube (B&K) are shown in figure 15 in which it is noted that the place of application of combined filters, before or after assembly of SACs fetches the same result. As Hampel + S-G (2) needs to be applied only once on the assembled value of SACs, it leads to a reduction in computation time. It is also observed that combined filters work much better than individual filters.

The result obtained by combined filtering (Hampel + S-G (2)), the result obtained from a standard experimental set-up of B&K, and the result obtained from the supplier of the materials has been compared in figure 16, and all these results are close to each other. This validates the developed experimental set-up, and the results obtained can be considered acceptable.

Melamine foam is removed from the sample holder and the experiment is conducted in a blank tube. The steps discussed above are repeated on these signals and the results obtained are compared with the reference [8], which also shows a good match and is shown in figure 17. Even though the tube is empty, still there is some sound absorption. This is explained by the definition of sound absorption which includes sound dissipated inside material and sound transmitted by the material in the medium behind it. As the absorbing material has been removed, this has nullified the dissipation part, but the steel backing has transmitted a fraction of sound into the other medium is responsible for the sound absorption.

The techniques discussed in previous sections are applied to glass wool samples which are available and used across the globe for noise control applications. Ten layers of glass wool, each of thickness 10 mm is piled up to make a 100 mm thick samples of diameter 100 mm and 29 mm each. The results

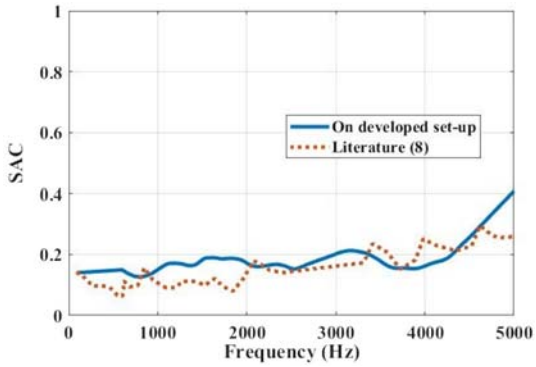


**Figure 17.** Sound absorption coefficients obtained in the developed setup without any sample compared with the result reported in the literature.

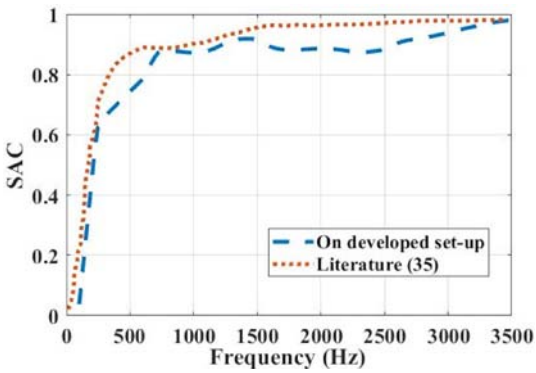


**Figure 18.** Sound absorption coefficients obtained in the developed setup with Glass wool samples compared with the result reported in the literature.

obtained are compared with reference [35], and the comparison is shown in figure 18 which shows a good degree of match.

The results produced by the tube has been counter verified by comparing the theoretical results obtained with empirical models for different fibers. The comparison of theoretical and experimental sound absorption coefficients for denim shoddy and waste jute fiber of different thicknesses and densities has been reported in their earlier work. The obtained results were matching quite well and found to be acceptable [36, 37].

## 7. Conclusions

Acoustics and noise control is a considerably young and exploring domain in which most of the technologies and theories have been developed in the second half of the previous century. This has severely limited the research base of this field as the cost involved in instrumentation is quite high. This study aims to open up the technology and provides well-validated literature addressing the concerns about data acquisition, mathematical equations implementation on these signals, and filtering techniques. The work has used the components which are available in most of the noise control laboratories, and thus limiting the repetition of elements which leads to saving some extra instrumentation cost. Two impedance tubes of different diameters 100 mm and 29 mm have been designed with fixed microphone spacing which estimates the sound absorption coefficients (SACs) as per standard ASTM-E-1050. The working frequency range response has been extracted from the results obtained through both these tubes. They are assembled and external noise is filtered out using a combination of customized filters. The results obtained are validated by different sources. Results of a 30 mm thick melamine foam are confirmed from the results obtained by a B&K impedance tube (Type 4206), and the result provided by the supplier. The results of a 100 mm thick glass wool and blank tube are validated from literature. The results are well accepted, and different sources of validation confirm the accuracy in different conditions. The fixed microphone spacing in a particular tube reduces the number of experiments by half, and with efficient filtering techniques, the correct low-frequency response is extracted.

## 8. Acknowledgements

The authors are thankful to the Department of Science and Technology-Government of India, for funding this project. They are also grateful to Prof. A R Mohanty (IIT Kharagpur) for providing the results of melamine foam on their experimental facility (B&K impedance tube, type 4206).

**Nomenclature**

| | |
|---|---|
| D | The diameter of the tube |
| c | Speed of sound |
| $f_u$ | Upper working frequency limit |
| S | Spacing between the microphones |
| $G_{12}$ | Cross power spectrum |
| $G_{11}$ | Auto power spectrum |
| s | Spacing between the microphones |
| k | Complex wave number |
| $k''$ | Attenuation constant |
| $\alpha$ | Sound absorption coefficient |
| K(s) | Window length in a Hampel filter |
| B&K | Brüel & Kjær |
| $H^I$ | The calibration transfer function of the tubes in standard configuration |
| $H^{II}$ | Calibration factor in swapped configuration |
| $H_c$ | Calibration factor |
| $H'$ | The transfer function of the absorptive sample |
| H | Corrected transfer function |
| R | Complex reflection coefficient |

| | |
|---|---|
| $l$ | Distance between the second microphone and sample |
| $k'$ | The real component of wavenumber |
| f | Frequency |
| Sigma (s) | Filter factor in a Hampel filter |
| SAC | Sound absorption coefficient |
| DAQ | Data acquisition system |

## References


[1] Tandon N 2000 Noise-reducing designs of machines and structures. *Sadhana* 25: 331-339

[2] Kinsler L E, Frey A R, Coppens A B, and Sanders J V 1999 *Fundamentals of Acoustics*, 4 edn. Wiley-VCH (New York), p. 340

[3] Munjal M L 2013 *Noise and Vibration Control*. World Scientific (Singapore). IISC lecture notes, Vol. 3, p 122

[4] Berendt R D and Schmidt Jr H A 1963 A portable impedance tube. *J. Acoustical Society of America* 35: 1049-1052

[5] ASTM E 1050-12. Standard test method for impedance and absorption of acoustic materials using a tube, two microphones, and a digital frequency analysis system

[6] Melo N, Morais M V, Nunes M A, and Oliveira A 2010 Development of an educational impedance tube: Experimental vibroacoustic characterization. *J. Acoustical Society of America* 128: 2446

[7] Kimura M, Kunio J, Huhmacher A S Cand Ryu Y 2014 A new high frequency impedance tube for measuring sound absorption coefficient and sound transmission loss. In: *Proceedings of 43rd International Congress and Exposition on Noise Control Engineering (INTER-NOISE), Melbourne, Australia.* 312

[8] Deshpande S P andRao M D 2014 Development of a low cost impedance tube to measure the acoustic absorption and transmission loss of materials. In: *2014 ASEE Annual Conference and Exposition, Indianapolis, Indiana*

[9] Tan W H, Ahmad R, Zunaidi N H D R and Cheng E M 2015 Development of an indigenous impedance tube. *Applied Mechanics and Materials.* 786: 149-155

[10] Krüger J andQuickert M 1997 Determination of acoustic absorber parameters in impedance tubes. *Applied Acoustics* 50: 79-89

[11] Feng L 2013 Modified impedance tube measurements and energy dissipation inside absorptive materials. *Applied Acoustics* 74: 1480-1485

[12] Oblak M, Pirnat M and Boltežar M 2018 An impedance tube submerged in a liquid for the low-frequency transmission-loss measurement of a porous material. *Applied Acoustics* 139: 203-212

[13] Suhanek M, Jambrosic K, and Domitrovic H 2008 Student project of building an impedance tube. *J. Acoustical Society of America* 123: 3616

[14] Rossing T D 1982 Experiments with an impedance tube in the acoustics laboratory. *American J. Physics* 50: 1137-1140

[15] Bolton J S and Compella M 2005 The three-microphone impedance tube. *J. Acoustical Society of America* 84: S96

[16] Uluisik C and Sevgi L 2012 A LabVIEW–based analog modulation tool for virtual and real experimentation. *IEEE Antennas and Propagation Magazine* 54: 246-254

[17] Du J, Li W and Guo J 2017 Design of LabVIEW based general data acquisition system. In: *IEEE 2nd Information Technology, Networking, Electronic and Automation Control Conference* 1235-1239

[18] Costas-Perez L C, Lago D, Farina J and Rodriguez-Andina J 2008 Optimization of an industrial sensor and data acquisition laboratory through time sharing and remote access. *IEEE Transactions on Industrial Electronics* 55: 2397-2404

[19] Ege Y, Kabadayi M, Kalender O, Coramik M, Citak H, Yuruklu E and Dalacali A 2016 A new electromagnetic helicalcoilgun launcher design based on LabVIEW. *IEEE Transactions on Plasma Science* 44: 1208-1218

[20] Umasthan M and Wallace A M 1996 Outlier removal and discontinuity preserving smoothing of range data. *IEEE Proceedings – Vision, Image and Signal Processing.* 143: 191-200

[21] Ferdowsi H, Jagannathan S and Zawodniok M 2014 An outlier identification and removal scheme for improving fault detection performance. *IEEE Transactions on Neural Networks and Learning Systems*.25: 908-919

[22] Dusmez S and Nourani M 2017 Remaining useful lifetime estimation for power MOSFETs under thermal stress with RANSAC outlier removal. *IEEE Transactions on Industrial Information* 13: 1271-1279

[23] Ramis J, Del R R, Alba J, Godinho L and Carbajo J 2014 A model for acoustic absorbent materials derived from coconut fiber. *Mater. Construcción* 64: 313

[24] Kino N 2012 A comparison of two acoustical methods for estimating parameters of glass fibre and melamine foam materials. *Applied Acoustics* 73: 590-603

[25] Cox T J and D'antonio P 2009 *Acoustic Absorbers and Diffusers: Theory, Design and Application*, 2 edn. CRC Press (London). p. 158

[26] Hampel D and Bradshaw J L 1980 Application of monolithic CMOS switched-capacitor filters and amplifiers for signal processing. *IEEE Transactions on Communications.* 2: 1828-1832

[27] Bhowmik S, Jelfs B, Arjunan S P, and Kumar D K 2017 Outlier removal in facial surface electromyography through Hampel filtering technique. *IEEE Life Sciences Conference (LSC)*: 258-261

[28] Pearson R K 2002 Outliers in process modeling and identification. *IEEE Transactions on Control Systems Technology* 10: 55-63

[29] Pearson R K, Neuvo Y, Astola J and Gabbouj M 2015 The class of generalized Hampel filters. In: *23rd European Signal Processing Conference (EUSIPCO)*: 2501-2505

[30] Zhang J X, Zhong Q H, Dai Y P and Liu Z 2003 A new denoising method based on wavelet transform and transforming Hampel filter. *SICE Annual Conference, IEEE*. 2: 2147-2151

[31] Seo J, Ma H and Saha T K 2018 On Savitzky-Golay filtering for online condition monitoring of transformer on-load tap changer. *IEEE Transactions on Power Delivery.* 33: 1689-1698

[32] Krishnan S R, Magimai-Doss M and Seelamantula CS 2013 A Savitzsky-Golay filtering perspective of dynamic feature computation. *IEEE Signal Processing Letters* 20: 281-284

[33] Krishnan S R and Seelamantula CS 2013 On the selection of optimum Savitzsky-Golay filters. *IEEE Transactions on Signal processing* 61: 380-391

[34] Schafer R W 2011 What is a Savitzsky-Golay filter? *IEEE Signal Processing Magazine*: 111-117

[35] Nenning B, Binois R, Dauchez N, Perrey-Debain E and Foucart F 2018 A transverse isotropic equivalent fluid model combining both limp and rigid frame behaviors for fibrous materials. *J. Acoustical Society of America* 143: 2089-2098

[36] Raj M, Fatima S and Tandon N 2019 Acoustical Properties of Denim Shoddy based Recycled Material. *INTER-NOISE and NOISE-CON Congress and Conference Proceedings* 259: 3528-33

[37] Raj M, Fatima S and Tandon N 2020 Recycled materials as a potential replacement to synthetic sound absorbers: A study on denim shoddy and waste jute fibers. *Applied Acoustics* 159: 1-13